International Journal of Mass Spectrometry 303 (2011) 181–190

Contents lists available at ScienceDirect

International Journal of Mass Spectrometry

journal homepage: www.elsevier.com/locate/ijms

Gas phase fragmentation of protonated esters in air at ambient pressure through ion heating by electric field in differential mobility spectrometry

X. An[a], G.A. Eiceman[a], J.E. Rodriguez[a], J.A. Stone[b]

[a] Department of Chemistry and Biochemistry, New Mexico State University, Las Cruces, NM 88003, United States
[b] Department of Chemistry, Queens University, Kingston, Ontario, Canada

ARTICLE INFO

Article history:
Received 28 January 2011
Accepted 29 January 2011
Available online 24 February 2011

Keywords:
Gas phase ion
Fragmentation
Effective temperature
Differential mobility spectrometry

ABSTRACT

A planar differential mobility spectrometer has been used to study the ions formed at atmospheric pressure by a series of n-alkyl carboxylic acid esters (M). MH^+ and M_2H^+ ions were present at low temperature. The combination of thermal energy and energy derived from collisional heating by acceleration in the asymmetric electric field caused ion decomposition at an effective temperature (T_{eff}) higher than ambient. The products were the protonated carboxylic acids, F^+. The electric field thresholds for the first observation of F^+ decreased as the temperature of the supporting gas atmosphere was increased and the rate, 1.5 °C per Townsend, was the same for all the esters. A measurable mass dependence for thresholds existed where the higher the molar mass for the ester of a given acid, the higher the required field. Although MH^+ is the well-established precursor of the protonated acid, an apparent direct formation of F^+ from M_2H^+ was observed even though no MH^+ was present in the spectrum. This is ascribed to T_{eff} being mass dependent. A field sufficient to raise a M_2H^+ to T_{eff} for dissociation to $MH^+ + M$, raises MH^+ to a higher T_{eff}, leading to its immediate decomposition.

1. Introduction

Collisional activation of ions, leading to their fragmentation, is an indispensible part of modern mass spectrometry for ion characterization [1]. The activation is made in general at low or extremely low pressure with ions accelerated in linear electric fields, as in magnetic sector and quadrupole instruments or with radio frequency fields as in ion traps. In all these techniques the dissociating ions are not in thermal equilibrium with a bath gas and hence are not at a defined temperature. The idea of an associated effective temperature for dissociation, T_{eff}, has led to much discussion, especially related to the kinetic method for the determination of proton affinities, where the relationship between enthalpy and free energy demands knowledge of the associated change in entropy [2–4]. Effective temperature for dissociation is somewhat difficult to define and its determination is therefore problematical.

If ions are dissociated under thermalized conditions with a bath gas, then T_{eff} is the temperature T, measured for the gas. Ion mobility spectrometers that operate at atmospheric pressure with linear electrostatic drift fields satisfy this condition [5]. Differential mobility spectrometers, which also operate at atmospheric pressure, employ a high asymmetric radio frequency field for ion separation. As a result, ions achieve, by collisional heating, an effective temperature T_{eff}, that is higher than the bath gas temperature [6,7]. Studies of the same reaction for an ion in both a linear mobility spectrometer and a differential mobility spectrometer should provide correlations to assign a value to T_{eff} for the reaction. A combination of two methods, field excitation in an ion trap and metastable ion decomposition in a sector instrument, to assign an effective temperature to an ionic reaction in vacuum has been reported [8]. In this paper, we describe a differential mobility spectrometry (DMS) investigation of possible ion decompositions for such a study in air at ambient pressure. The decomposition of alkyl ester ions, protonated molecules (MH^+) and proton bound dimers M_2H^+, was chosen since the calculated required energies, <130 kJ mol^{-1} [9] are compatible with the upper operating temperature available with a linear ion mobility spectrometer. For example, linear ion mobility spectrometers operated at ambient pressure and known temperature were used to provide kinetic and thermochemical data pertinent to the decomposition of cluster ions with dissociation energies from 90 to 130 kJ mol^{-1} [10,11].

An essential parameter for defining conditions in a mobility spectrometer is the ratio of the electrostatic field strength to the number of molecules per unit volume, E/N, since T_{eff} is determined by both E and N [12]. A convenient unit, with E in V cm^{-1} and N in molecule cm^{-3}, is the Townsend (Td); 1 Td = 1×10^{-17} V cm^2. The drift velocity (v_d) of an ion swarm, derived from measurement of time of drift (t_d) through a drift region of known length, is described as the mobility coefficient, K, when v_d is normalized to the electric field strength (Eq. (1)).

$$K = \frac{v_d}{E} \quad (1)$$

1387-3806/$ – see front matter © 2011 Elsevier B.V. All rights reserved.
doi:10.1016/j.ijms.2011.01.031

The value of K is determined principally by the collision cross section and reduced mass of the ion and supporting gas molecules [12]. Ions present in a supporting gas at atmospheric pressure with E in the range 200–500 V cm^{-1} (0.6–2.1 Td), the usual fields in a linear mobility spectrometer, are said to be under low field conditions. The drift motion of ions induced by the electrostatic field contributes energy that is negligible compared with thermal energy [5,12] and at constant temperature K is constant, independent of electrostatic field, under low field conditions (E/N < 10 Td).

In the past twenty years, instruments and methods to characterize ions under atmospheric pressure and high field conditions (E/N > 10 Td), where K is usually field dependent, have been developed as field asymmetric mobility spectrometry (FAIMS) or DMS [6,13–15]. In a differential mobility spectrometer ions are moved in a flowing gas, the transport gas, through a transverse high frequency asymmetric electric field, the separation field. In one cycle, the integrated field intensity over time at the high field is equal to the integrated intensity over time at the low field. For example, a high field of +176 Td is followed by a low field of −59 Td with a dwell time at high field one third that at low field. Ions with field dependent mobility coefficients are displaced toward a wall of the analyzer where they are neutralized. An Ion can be maintained in the transport gas and prevented from reaching the wall by a small DC field superimposed on the asymmetric field; the ion passes to a detector, commonly a Faraday plate or, increasingly, a mass spectrometer. When this DC field, the compensation field, is scanned, the differential mobility spectrum of all ions at their characteristic compensation fields is generated.

The dependence of ion mobility on the electric field is described by Eq. (2):

$$K\left(\frac{E}{N}\right) = K(0)\left[1 + \alpha\left(\frac{E}{N}\right)\right] \quad (2)$$

where $K(0)$ is the mobility coefficient under the low field condition and $\alpha(E/N)$ is an alpha (α) function equal to $\alpha_2(E/N)^2 + \alpha_4(E/N)^4 + \cdots$, where α_2, α_4, ... are ion dependent coefficients. Ions gain and lose energy by collision but accumulate energy above ambient as they are accelerated in the separation field. The magnitude of the change in $K(E/N)$ with change in E is attributed to the association and dissociation of weakly solvating ligands such as water and other ambient molecules, and from changes in the potential of interaction with the surrounding atmosphere during low and high field portions of the asymmetric waveform of the separating field [6,16–18]. Dissociation of non-covalently bound ions and/or of core ions may occur through the increase in internal energy of the ions gained from the separating field, as has been demonstrated with protonated diphenyl methane and dibenzyl, each of which fragmented by loss of benzene [7] and by the fragmentation of methylsalysilate$^{\bullet}O_2^-$ adducts which lose HO_2 [16].

We report a study of the fragmentation of alkyl ester ions in a differential mobility spectrometer. The required activation energy was supplied by a combination of instrument heat and electric field. A homologous series of n-alkyl acetates, from n-propyl to n-hexyl was employed in order to compare the decomposition of esters of the same acid with increasing molar mass. Studies with propyl propanoate and propyl butanoate allowed observation of the effect of a different acid with the same alkyl group as did ethyl propanoate and ethyl hexanoate. The chemicals chosen for the study are straight chain acid esters which readily protonate at ambient pressure without decomposing in a beta ion source. The protonated molecules form relatively weak hydrogen bonds with the neutral molecules.

2. Experimental

2.1. Instrumentation

Experiments were performed with three instruments: a differential mobility spectrometer fed by a constant vapor generator; a gas chromatograph with DMS detection; and a DMS analyzer interfaced to a triple quadrupole mass spectrometer. A Sionex Corporation (Bedford, MA, USA), model SVAC differential mobility spectrometer was used for DMS and GC/DMS studies. The operation of this planar differential mobility spectrometer has been described in detail [18]. The SVAC was equipped with an ion source containing 5 mCi ^{63}Ni and a Sionex SVAC Software Expert data acquisition system (Sionex Corp). The transport gas was 500 mL min^{-1} of air, purified by 13× molecular sieve, to a moisture level of 0.3 ppm$_v$, as measured by a Moisture Image Series 2 (Panametrics, Inc. Waltham, MA, USA) at the exhaust of the DMS analyzer. The residence time of an ion in the analytical volume at this transport gas flow rate is 2.5 ms. A vapor generator was built to introduce ester vapors, when required, at controlled, appropriate concentrations.

The same DMS instrument was used for GC/DMS studies with a Hewlett Packard Series II 5890 gas chromatograph (Avondale, PA, USA) equipped with a 30 m RTX®-200 capillary column and heated transfer line between the GC oven and the DMS analyzer. GC/DMS experiments assured sufficient purity of samples and provided a first assessment of electric field-induced ion decomposition. Operating conditions were: initial temperature 28 °C for 3 min; temperature ramp, 4 °C/min; final temperature 120 °C; splitless injection with an injector temperature of 200 °C. The carrier gas was high purity nitrogen at 1 mL/min.

A second DMS analyzer, for the DMS/MS/MS experiments, was built in house and equipped with SVAC electronics and the same data acquisition system [16,17]. The planar separation region consisted of two ceramic plates with gold plated copper-base electrodes. The electrodes, stabilized in an aluminum metal body to which a 10 mCi of ^{63}Ni ion source was attached, had dimensions: length, 13 mm; width, 5 mm; height, 0.5 mm. Both DMS instruments were operable in the temperature range from ambient to 150 °C and had separation field frequencies of 1.2 MHz. The mass spectrometer was a model API III (PE-SCIEX Toronto, Ontario, Canada) and has been described in detail [19]. The transport gas was 2.0 L/min of ultra high purity nitrogen (Argyle Welding Company, Las Cruces, NM, USA) passed through 13× molecular sieve. Samples for DMS/MS/MS studies were prepared using the same constant flow vapor generator as used for the stand-alone DMS studies.

2.2. Reagents and samples

Methyl acetate, n-propyl acetate, n-butyl acetate, n-pentyl acetate, n-hexyl acetate, ethyl propanoate, ethyl hexanoate, propyl propanoate, propyl butanoate, and 2,4-dimethyl pyridine (DMP), purchased from Aldrich (Milwaukee, WI, USA), were of the highest available purity and were used as received. Two stock solutions were prepared for chromatographic analyses, one was a mixture of the five acetates in methylene chloride (~0.87 ng/μL for each): the other was a mixture of the other four esters in methylene chloride (~0.87 ng/μL for each). A solution of DMP (0.23 ng/μL) was also made up in methylene chloride.

2.3. Procedures

The effect of energy gained from the collisional heating of ions in the separation field was studied first by GC/DMS analysis at different separation fields with a fixed DMS analyzer temperature of 100 °C. The separation field was incremented in 5.1 Td steps from 71 Td to 152 Td and at each step the compensation field was

scanned at 1 Hz from −4.4 Td to +1.5 Td in 0.06 Td steps. A solution volume of 1 μL was injected into the chromatograph and DMS spectra were obtained continuously as the chromatographic column temperature was programmed. A topographic plot of ion intensity as a function of compensation field and retention time was generated at each separation field. For DMP, the same procedure was followed except that the DMS analyzer was at 50 °C.

The effect of the combination of DMS analyzer temperature and separation field on ion decomposition was carried out for each ester at a constant concentration in the transport gas provided by the vapor generator. The DMS analyzer temperature was fixed and the separation field was scanned in 100 s from 59 Td to 176 Td in 1.2 Td intervals and at each field a DMS spectrum was obtained with compensation field scanning from −5.0 to +1.7 Td. A topographic plot of ion intensity as a function of separation field and compensation field was obtained for analyzer temperatures from 30 °C to 150 °C in 10 °C steps. Product ions were identified for each ester in a separate series of experiments by DMS/MS/MS analysis with the DMS analyzer at a temperature of 100 °C.

3. Results and discussion

3.1. 2,4-Dimethyl pyridine (DMP)

The ion chemistry of DMP that occurs in an atmospheric pressure ^{63}Ni ionization source operating at atmospheric pressure is well-described. The protonated molecule $(DMP)H^+$ is first formed by proton transfer from the reactant ion $(H_2O)_nH^+$ and subsequently the proton bound dimer $(DMP)_2H^+$ may form by association of $(DMP)H^+$ with DMP at sufficiently elevated vapor concentrations [10]. The ion $(DMP)_2H^+$ dissociates thermally at 90 °C ($k = 2.4 \times 10^2\ s^{-1}$) in the absence of DMP. This simple ion chemistry (Eqs. (3)–(5)) renders DMP an ideal chemical to use to observe the heating effect of the separation field on ion dissociation, uncomplicated by ion fragmentation.

$$(H_2O)_nH^+ + DMP \rightarrow nH_2O + (DMP)H^+ \quad (3)$$

$$(DMP)H^+ + DMP \rightarrow (DMP)_2H^+ \quad (4)$$

$$(DMP)_2H^+ \rightarrow (DMP)H^+ + DMP \quad (5)$$

Results from GC/DMS studies are shown in the topographic plots of Fig. 1 for DMP at six separation fields with a fixed analyzer temperature of 50 °C. Both the separation field and the compensation field are normalized to the transport gas concentration, i.e. E/N in Td units. The reactant ion peak (RIP) maximum appears at a compensation field of −0.53 Td at the lowest separation field of 71 Td. The RIP becomes less intense and moves to more negative values with increasing separation field, −0.76 Td, −0.94 Td and −1.1 Td at separation fields of 82 Td, 87 Td and 92 Td respectively and is outside the scale of Fig. 1e and f. The contour lines of the RIP peak in Fig. 1a show the decrease in intensity of $(H_2O)_nH^+$ when DMP elutes and this diminution and subsequent return of intensity maps the DMP chromatographic elution profile. At 71 Td, and a retention time of 12.15 min., the DMP concentration is a maximum and new ion intensity is seen that extends from −0.3 to +0.2 Td on the compensation field scale. At an elution time of 14 min. in the tail of the chromatographic peak, where the DMP concentration is extremely low, ion intensity is in a narrow region around −0.17 Td. Two maxima in ion intensity develop at high DMP concentration as the separation field is increased. At 92 Td for example, the maxima are located at compensation fields of −0.24 Td and 0.05 Td. The ions represented by these maxima were identified by DMS/MS/MS as, respectively, $(DMP)H^+$ and $(DMP)_2H^+$. The intensity of $(DMP)_2H^+$ relative to $(DMP)H^+$ decreases with increasing separation field until at 142 Td only $(DMP)H^+$ remains. In addition, the absolute intensities of both ions decrease with increases in separation field; this is understood to be a loss in transmission efficiency, for differential mobility spectrometers with planar configurations, through neutralization by collisions of ions on walls of the analyzer. Increases in separation voltage lead to increases in collisions for ions not in the centre of the flow channel of the analyzer. The decrease in intensity is generally less for heavier, less mobile ions.

Mobility bias in transmission will favor retention of the heavier, less mobile $(DMP)_2H^+$, and the decrease in intensity of this ion relative to that of $(DMP)H^+$ is particularly apparent in the graphs for 102 Td and 142 Td. The disappearance of $(DMP)_2H^+$ before $(DMP)H^+$ must arise from the dissociation of the dimer after it acquires sufficient energy from the separating field. The lowest energy process for the dissociation of $(DMP)H^+$, observed in CAD mass spectra is loss of methyl to give m/z 93. This ion would have been detected if it had been formed since it has a mass of the same magnitude as $(DMP)H^+$ which was readily seen. Its absence shows that a differential mobility detector separation field of 142 Td did not supply sufficient energy for the fragmentation of $(DMP)H^+$.

Several conclusions may be drawn from the above results: (1) The ion chemistry of DMP illustrated by Fig. 1 is as summarized by Eqs. (3), (4)and (5). (2) $(DMP)_2H^+$ formed in abundance in the source (Eq. (4)) at low temperature is completely dissociated by activation in the highest separation field. (3) No fragmentation of $(DMP)H^+$ occurs. (4) The separation of $(DMP)H^+$ and $(DMP)_2H^+$ ions is improved with increased separation field and good resolution is observed above 87 Td. (5) The compensation field required to transmit the heavier ion $(DMP)_2H^+$ changes very little, from a compensation field of 0 Td to 0.05 Td when the separation field changes from 87 Td to 142 Td. By contrast, $(DMP)H^+$ moves from −0.13 Td at a separation field of 71 Td to −0.24 Td at a separation field of 102 Td and then folds back to −0.07 Td at 142 Td, showing that the α value (Eq. (2)) has maximized and then decreased.

3.2. Methyl acetate

The CAD spectrum of protonated methyl acetate shows loss of methanol as the lowest energy process (Eq. (6)) with a calculated enthalpy requirement of 156 kJ mol^{-1} [9].

$$(CH_3COOCH_3)H^+ \rightarrow CH_3CO^+ + CH_3OH \quad \Delta H^\circ = 156\ kJ\ mol^{-1} \quad (6)$$

The energetic requirements for the dissociation of all other protonated n-alkyl esters are lower. For example, that for n-propyl acetate, which decomposes to protonated acetic acid and propene (Eq. (7)), is lower by 54 kJ mol^{-1} [9].

$$(CH_3COOC_3H_7)H^+ \rightarrow CH_3COOH_2^+ + C_3H_6 \quad \Delta H^\circ = 102\ kJ\ mol^{-1} \quad (7)$$

In order to determine whether the decomposition of $(CH_3COOCH_3)H^+$ was possible by collisional activation in the separation field, a relatively large concentration of methyl acetate was employed in a GC/DMS study with an ionization source temperature of 100 °C. Fig. 2 shows that this high concentration causes the almost complete disappearance of the RIP at a separation field of 82 Td, and the appearance of the proton bound dimer, $(CH_3COOCH_3)_2H^+$, which was identified by GC/DMS. The chromatographic elution profile of the ester is defined by the contours of the $(CH_3COOCH_3)_2H^+$ intensity at a compensation field of −0.07 Td while $(CH_3COOCH_3)H^+$ at −0.47 Td shows significant intensity only at the leading and trailing edges of the chromatographic peak where the ester concentration is very low. There is good resolution between the two ion intensities. Since mobility bias in transmission favors $(CH_3COOCH_3)_2H^+$, its loss of relative intensity with increasing separation field, particularly apparent in plots obtained at 105 Td to 142 Td, arises from another source, namely, dissociation and disappearance of this ion after

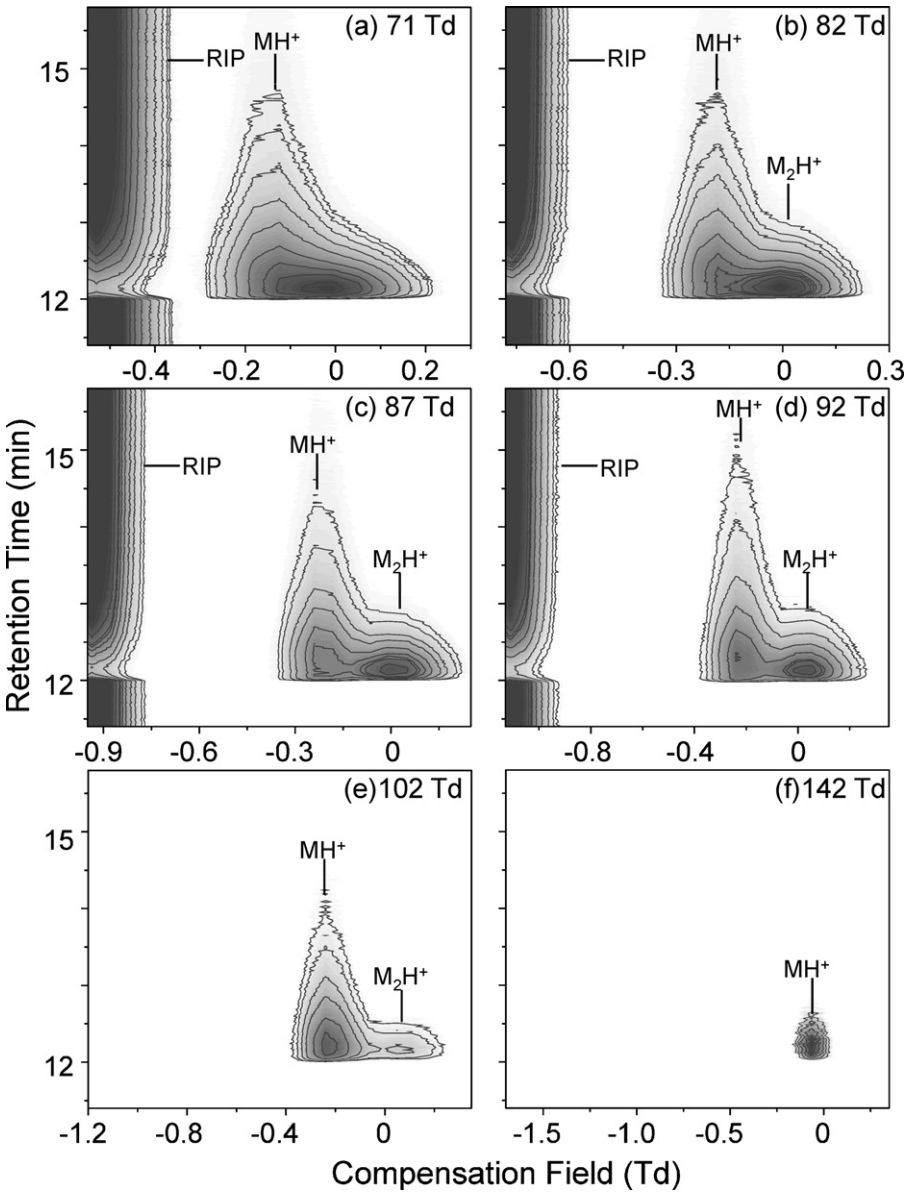

Fig. 1. GC/DMS topographic plots for 1 μL of a 0.23 ng/μL DMP solution. DMS analyzer temperature 50 °C; separation fields: (a) 71, (b) 82, (c) 87, (d) 92, (e) 102, (f) 142 Td. M_2H^+ is $(DMP)_2H^+$, MH^+ is $(DMP)H^+$, and RIP is $(H_2O)_nH^+$.

activation by energy gained in the separating field. After 105 Td, the proton bound dimer is not present and only $(CH_3COOCH_3)H^+$ is seen. No evidence for fragmentation of $(CH_3COOCH_3)H^+$ was found. Fig. 2 illustrates the dissociation of a proton bound ester dimer with energy gained from the separation field with good resolution between reactant and product ions. These results for methyl acetate are to be compared with those for the other esters described below.

3.3. *n*-Alkyl acetates

The GC/DMS spectra shown in Fig. 3 for n-propyl acetate at six different separating fields are representative of those obtained with the other acetates. The RIP signal is out of the range of the plotted compensation field but its behavior was identical to that described for the experiments with DMP and methyl acetate. The ions in the spectra were identified by DMS/MS/MS as: $(CH_3COOC_3H_7)_2H^+$ (M_2H^+), $(CH_3COOC_3H_7)H^+$ (MH^+), and $(CH_3COOH)H^+$ (F^+). The single peak at a separation field of 82 Td is resolved into two peaks at 94 Td, MH^+ and M_2H^+ at the respective compensation fields of −0.21 Td and 0.12 Td. F^+ is present at −0.62 Td with very low intensity with this separation field. F^+ increases in relative intensity with increasing separation field until at 164 Td it is the remaining ion.

Fig. 4a–c show the DMS/MS mass spectra for propyl acetate obtained at three different separation fields. At 70 Td, $(H_2O)_nH^+$ is present at m/z 73 and m/z 55 ($n = 4$ and 3 respectively). The concentration of the ester was constant but was not measured; it was obviously lower than that used to obtain the data for Fig. 2. A very low intensity of m/z 73 remains at 117 Td, with m/z 55 at too low an intensity to be graphed. At 70 Td, M_2H^+ (m/z 205) is the major ion and MH^+ is present as the di-hydrate (m/z 121) and tri-hydrate (m/z 139). No hydrate of M_2H^+ was observed. At 117 Td, the peaks of the di- and mono-hydrates of F^+ at m/z 97 and 79 are much more intense than m/z 121. M_2H^+, however, is still the major peak. Only the F^+ hydrate peaks are present at 164 Td. The identification of m/z 97 as the dihydrate of protonated acetic acid is shown in the CAD spectrum of Fig. 4d. Sequential loss of the two water molecules fol-

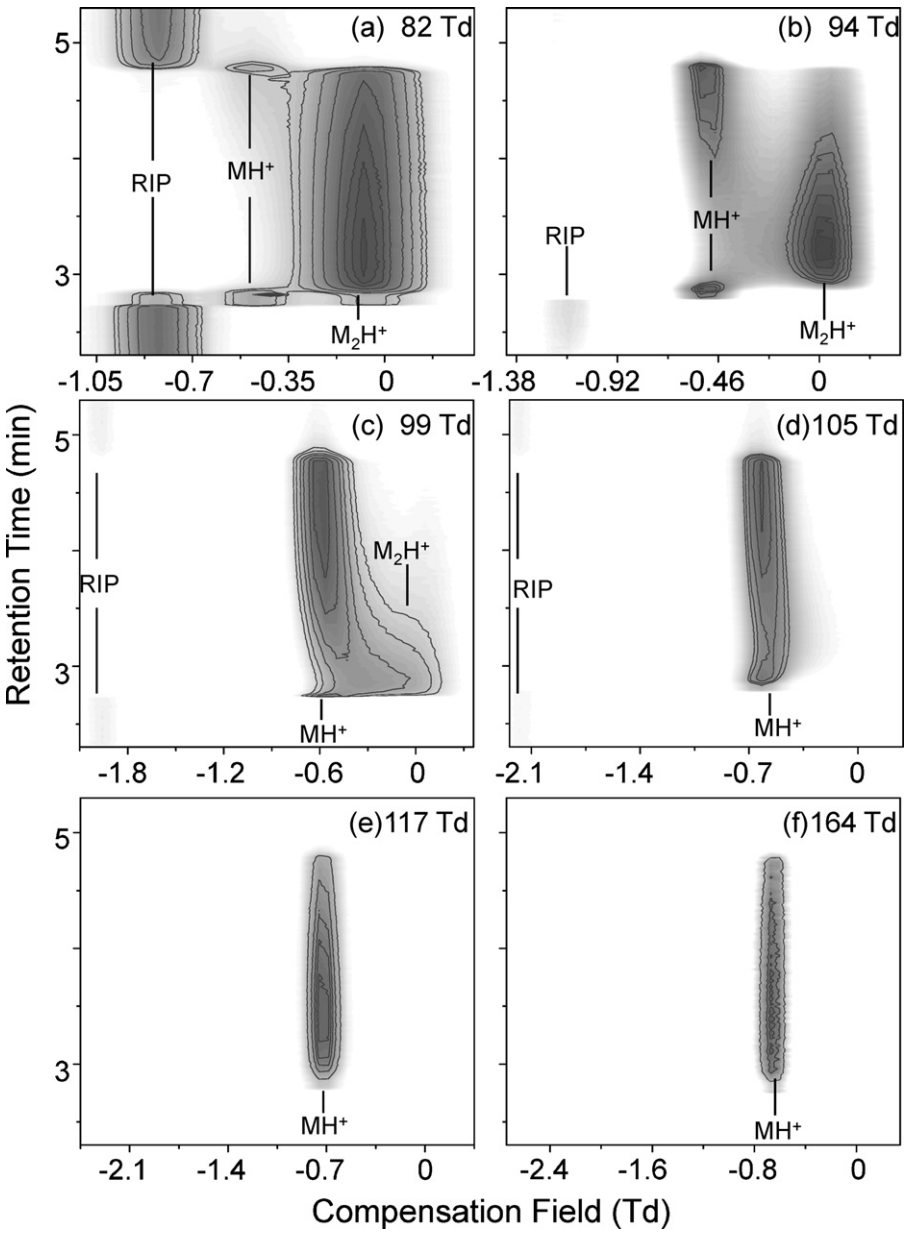

Fig. 2. GC/DMS topographic plots for 0.76 μg methyl acetate. DMS analyzer temperature 100 °C; separation fields: (a) 82, (b) 94, (c) 99, (d) 105, (e) 117, (f) 164 Td. M_2H^+ is $(CH_3COOCH_3)_2H^+$, MH^+ is $(CH_3COOCH_3)H^+$, RIP is $(H_2O)_nH^+$.

lowed by loss of a third water molecule gives *m*/*z* 43, the acetyl cation CH_3CO^+.

There are two remarkable differences between the behavior shown by propyl acetate in Fig. 3, confirmed by Fig. 4, and that shown by methyl acetate in Fig. 2. First, MH^+ of methyl acetate does not decompose further even at a separation field of 164 Td whereas MH^+ of propyl acetate does, and second, M_2H^+ of propyl acetate survives to higher field than does MH^+. The reverse is the case for methyl acetate. Experience with DMP and methyl acetate, as described above, proves that the upper separation field for MH^+ viability for propyl acetate being lower than for M_2H^+ is not due to transmission loss but is due to its further decomposition. The other acetates, n-butyl to n-hexyl, behaved in the same manner as n-propyl, in that the proton bound dimer, M_2H^+, although decreased in intensity as the separation field was increased, still remained after the protonated molecule MH^+ was no longer observed. F^+ was the only ion present in the spectrum at the highest field. The first appearance of F^+ and the last observation of MH^+ for each ester occurred at approximately the same field but the fields were slightly different for the different esters.

Experiments with propyl propanoate, propyl butanoate, ethyl propanoate and ethyl hexanoate by GC/DMS and DMS/MS/MS produced results similar to those obtained with the acetates. The ions observed with each ester were M_2H^+, MH^+ and F^+, the corresponding protonated acid. Again, as the separation field was increased, M_2H^+ was present in the spectrum at higher fields than MH^+. The extent of protonated acid formation as judged by relative ion intensities at the same separation field and mobility spectrometer temperature was in the order, propyl propanoate > propyl butyrate > ethyl propanoate > ethyl hexanoate. The behavior of the esters as a function of separation field was investigated further with a stand-alone differential mobility analyzer and a constant concentration of ester in the transport gas.

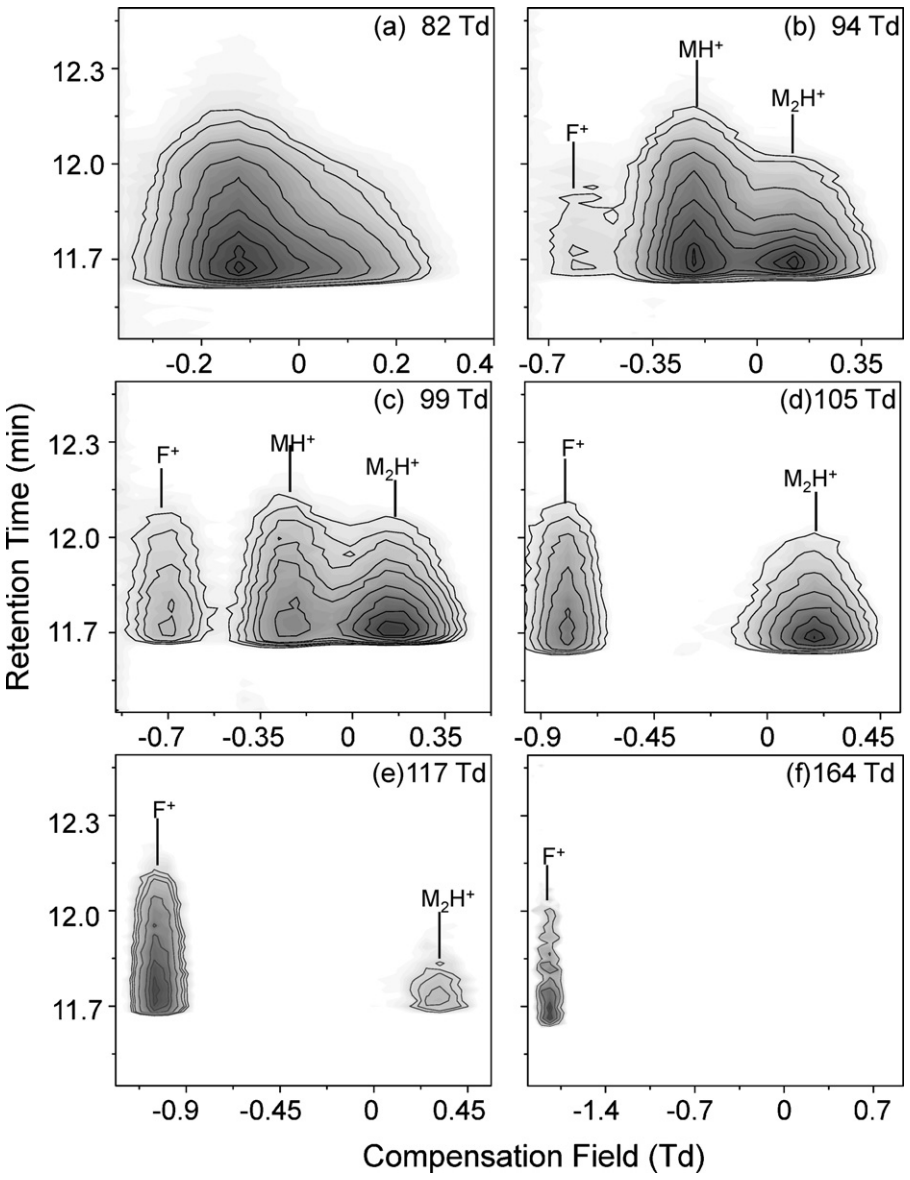

Fig. 3. GC/DMS topographic plots for 1 μL of 0.87 ng/μL propyl acetate. DMS analyzer temperature 100 °C; separation fields: (a) 82, (b) 94, (c) 99, (d) 105, (e) 117, (f) 164 Td. M_2H^+ is $(CH_3COOC_3H_7)_2H^+$, MH^+ is $(CH_3COOC_3H_7)H^+$, and F^+ is $(CH_3COOH)H^+$.

3.4. Thresholds for protonated ester decomposition

The activated decompositions of M_2H^+ and MH^+ are due to the combination of thermal energy and the energy acquired from the separation field. Experiments were carried out to further investigate the effect of this summation on the different esters. DMS experiments, with the same constant concentration of ester supplied to the transport gas by a vapor generator were carried out to investigate the behavior of the esters as a function of separation field. A dispersion plot, a topographic plot of ion intensity as a function of compensation field and separation field was generated for each ester. A typical result, for propyl acetate obtained with a transport gas temperature of 100 °C, is shown in Fig. 5.

At the lowest separation field, 59 Td, there is a single peak with a maximum at a compensation field of 0.08 Td. A small increase in separation field results in a discernable first appearance of the RIP. At higher fields, separation of the reactant ions from the others is complete and the RIP disappears at 117 Td. MH^+ first shows separation from M_2H^+ at 82 Td, but persists only to 109 Td. The decomposition of MH^+, giving F^+, is first apparent at 85 Td and its intensity increases with increasing field. M_2H^+ persists to a field of about 125 Td while F^+ is still present at the highest field. The normalized intensities of M_2H^+, MH^+ and F^+, excluding the RIP ions, are plotted as a function of separation field in Fig. 6a. The figure shows equal intensities of MH^+ and M_2H^+ at the lowest field, 80 Td, which is a function of poor resolution rather than being an accurate representation of relative intensities. The important conclusion to be drawn from the figure is that the relative intensity of MH^+ decreases monotonically and disappears at 110 Td. The relative intensity of M_2H^+ maximizes and decreases as F^+ increases and becomes the dominant ion at the highest fields.

The DMS/MS results of Fig. 6b for propyl acetate confirm the DMS results of Fig. 6a. At the lowest separation field, M_2H^+ is present with much higher intensity than MH^+. The salient points in Fig. 6b, with those for Fig. 6a in brackets, are: M_2H^+ maximizes at 94 Td (102 Td); MH^+ disappears at 117 Td (110 Td); F^+ first appears at 82 Td (85 Td); M_2H^+ and F^+ are equal at 120 Td (113 Td); and M_2H^+ disappears at 140 Td (132 Td). Both M_2H^+ and MH^+, although unresolved in Fig. 5 are present in the mass spectrum at a field of 59 Td. Only F^+ remains at the highest fields.

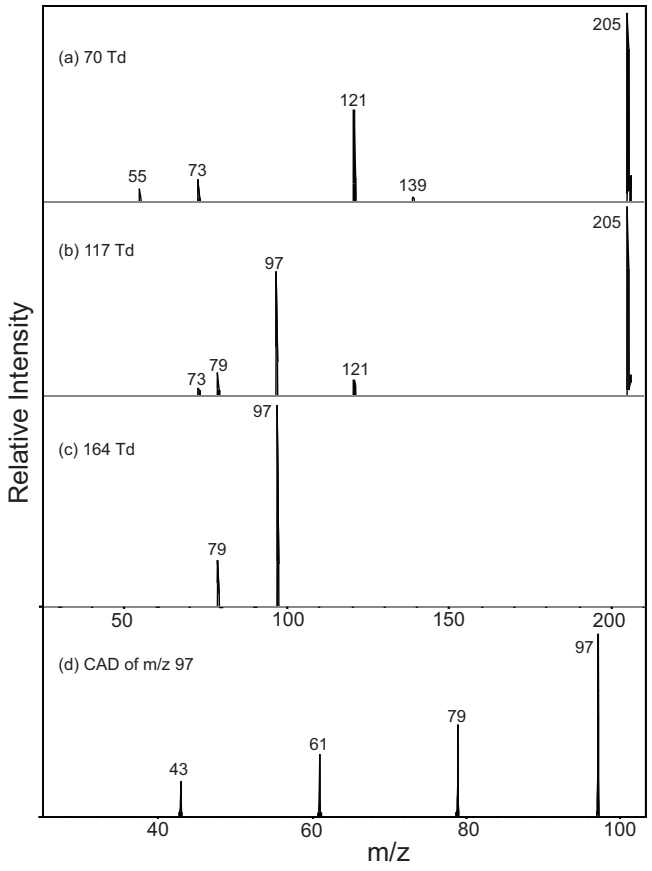

Fig. 4. DMS/MS spectra for propyl acetate with separation fields of (a) 70 Td, (b) 117 Td and (c) 164 Td. The peaks are: *m/z* 205, M_2H^+; *m/z* 103, 121 and 139, MH^+, $MH^+(H_2O)$ and $MH^+(H_2O)_2$; *m/z* 55 and 73 $H^+(H_2O)_3$ and $H^+(H_2O)_4$; *m/z* 61, 79, 97, $CH_3COOH_2^+$, $CH_3COOH_2^+(H_2O)$, and $CH_3COOH_2^+(H_2O)_2$; and *m/z* 43, CH_3CO^+. The CAD spectrum of the hydrate of protonated acetic acid with *m/z* of 97 for a DMS analyzer temperature of 100 °C.

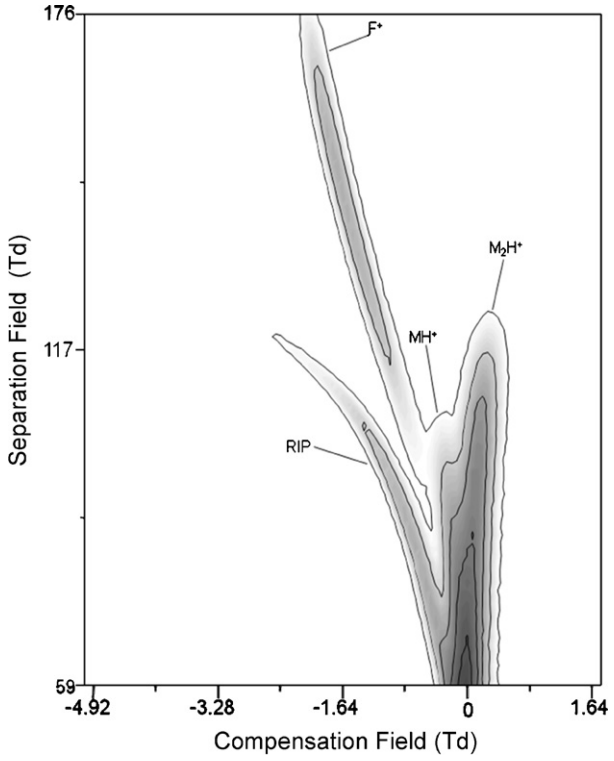

Fig. 5. Dispersion plot for propyl acetate at a DMS analyzer temperature of 100 °C. The M_2H^+ is $(CH_3COOC_3H_7)_2H^+$, MH^+ is $(CH_3COOC_3H_7)H^+$, F^+ is $(CH_3COOH)H^+$ and RIP is $(H_2O)_nH^+$.

Ion decomposition in the separation field is brought about by the conversion of translational energy acquired from acceleration in the field into internal energy. This energy is in addition to thermal energy determined by the transport gas temperature. By raising the temperature of the transport gas, the energy required from the field for ion decomposition should be decreased. The decomposition of M_2H^+ to $MH^+ + M$ is not a suitable reaction for a DMS investigation of this phenomenon since there is no spectral resolution at the energy threshold. However, the formation of F^+, which has a determinable threshold as seen in Fig. 5, is a suitable reaction.

Dispersion plots, such as that for propyl acetate in Fig. 5, were obtained for all the esters at temperatures from 30 °C to 150 °C in 10 °C increments and the separation fields required for the first appearance of the protonated acid F^+ at each temperature were determined. The results, separation field threshold versus DMS analyzer temperature, are shown in Fig. 7. There is a clear distinction between the results for the acetates and those for the esters of the higher acids; lower fields are required for the first appearance of F^+ from the acetates than from the esters of the higher carboxylic acids. The separation field for first observation of protonated acetic acid at all temperatures increases in the order propyl < butyl < pentyl < hexyl, i.e. in order of increasing ionic mass.

Some of the kinetic energy the ions gain by acceleration in the separation field is converted into internal energy by collision with the transport gas. Energy can also be lost in a collision so that at a given high field a balance should be attained between energy gain and loss. In the asymmetric separation field the energy content of an ion at high field will be greater than that at the low field portion of the cycle and the threshold field for first observation of F^+ will occur at the maximum of the high field portion of the cycle. If the same activation energy is required for decomposition, independent of alkyl chain length, then the required high field that scales with ion mass is determined by the total energy requirement to attain the same T_{eff} for decomposition. The mass dependence of the threshold for MH^+ decomposition correlates with an increasing number of vibrational modes in the decomposing MH^+, i.e. with the heat capacity of the ion.

The correlation with mass of the increasing threshold for the appearance of F^+ from MH^+ is not the whole picture, since the threshold for the ester of a higher acid is always greater than that of an isobaric acetate ion. For example, the threshold for propyl propanoate is greater than that for butyl acetate and the threshold for ethyl hexanoate is greater than that for hexyl acetate. The MH^+ ions of the ethyl esters, the propanoate and hexanoate, appear particularly stable. MH^+ from ethyl propanoate is more stable in the separation field than is MH^+ from propyl propanoate and MH^+ from ethyl hexanoate is extremely stable. Unfortunately, no experimental data is available for ethyl acetate, which might strengthen this conjecture regarding the ethyl esters. The relationship between the separation field required for the dissociation of MH^+ at a given temperature and the nature of the ester is obviously complex since the variables of size of alkyl group and acid groups are melded with ionic mass. Further experimentation with a larger set of higher esters, for example propanoates and butanoates is desirable.

The plots of separation field versus temperature in Fig. 7 are linear with slopes that are all very similar and show no bias with respect to the molar mass of the ester or to the nature of the acid and alkyl group. The average slope is -0.68 ± 0.06 Td °C^{-1}. That is, for every 1 Td increase in separation field strength the required temperature for the appearance of F^+ decreases by 1.5 °C.

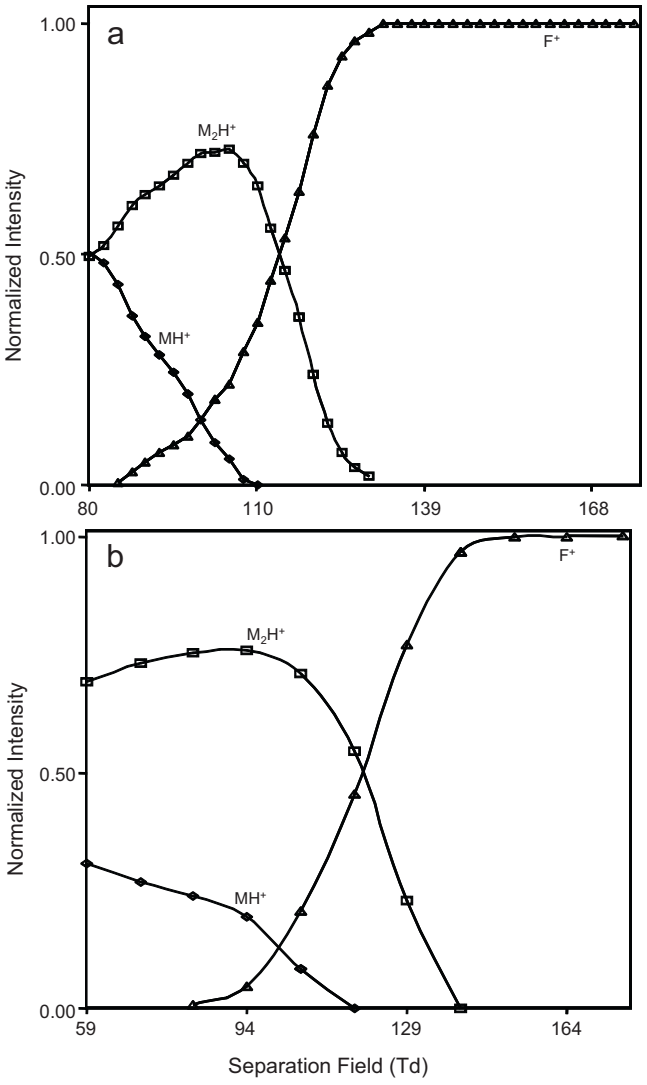

Fig. 6. The normalized ion intensities of propyl acetate obtained by (a) DMS and (b) DMS/MS at a DMS temperature of 100 °C. The MH^+ is $(CH_3COOC_3H_7)H^+$ (including hydrates), M_2H^+ is $(CH_3COOC_3H_7)_2H^+$, and fragment $CH_3COOH_2^+$ (including hydrates) normalized to the total ion intensity, against separation field of DMS (Legends: MH^+ "◊";M_2H^+ "□"; fragment "△").

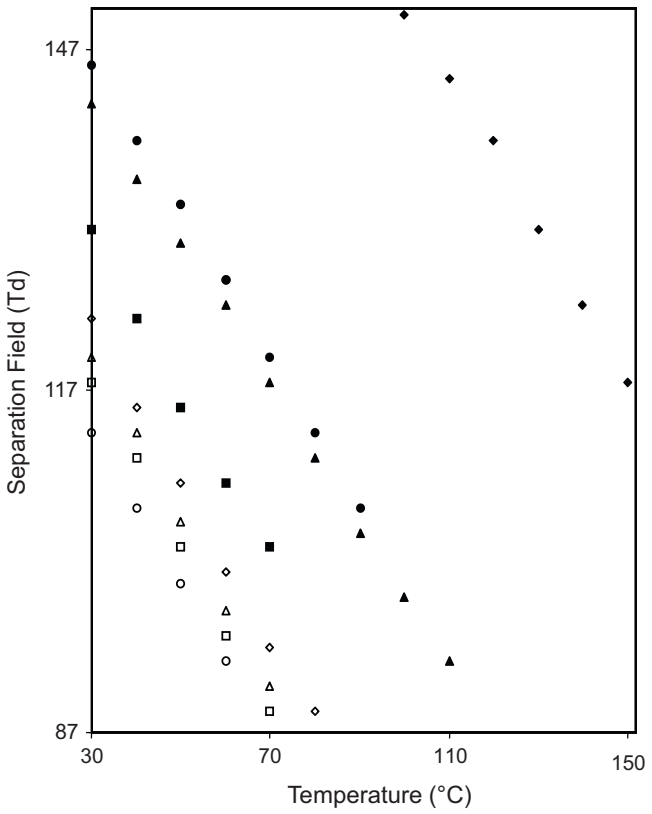

Fig. 7. Separation voltages for the first observation of a formation of protonated acid versus DMS temperature. Propyl acetate "○", butyl acetate "□", pentyl acetate "△", hexyl acetate "◊", propyl propionate "■"" propyl butyrate "▲", ethyl propionate "●", and ethyl hexanoate "♦".

3.5. Mechanism of ion decomposition

The ions observed with each of the esters over the range of differential mobility spectrometer temperatures and separation electric fields are M_2H^+, MH^+ and F^+. The enthalpy change for the dissociation of M_2H^+ to $MH^+ + M$ (Eq. (8)) is expected to be almost identical for each ester.

$$M_2H^+ \rightarrow MH^+ + M \quad (8)$$

Symmetrical proton bound dimers with $O\cdots H^+\cdots O$ bonds are predicted to have essentially the same hydrogen bond energy of $\sim 129 \pm 8\,kJ\,mol^{-1}$ [20,21]. This prediction is borne out by pulsed high pressure mass spectrometric determinations for the dimers of ethyl acetate and propyl acetate that have the same bond energy, $122\,kJ\,mol^{-1}$ [22]. The decomposition of the protonated ester to give protonated carboxylic acid is actually less endothermic than for the dissociation of the dimer for any ester other than methyl acetate. For example, the decomposition of propyl acetate to give protonated acetic acid and propene (Eq. (7)) is calculated to be endothermic by $102\,kJ\,mol^{-1}$ while for protonated ethyl acetate, decomposition giving acetic acid and ethene (Eq. (9)) is endothermic by $119\,kJ\,mol^{-1}$ [9].

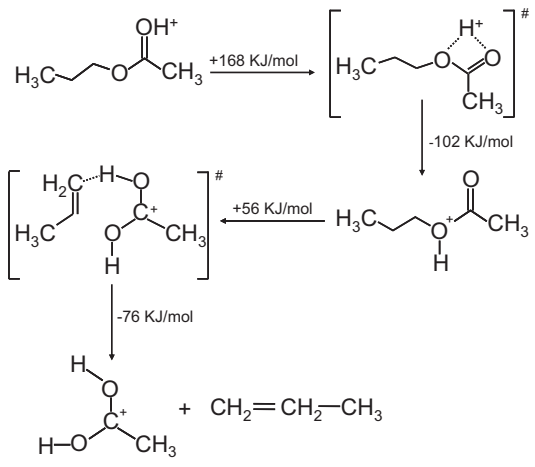

Scheme 1.

$$CH_3COOC_2H_5H^+ \rightarrow CH_3COOH_2^+ + C_2H_4 \quad \Delta H^\circ = 119\,kJ\,mol^{-1} \quad (9)$$

The most stable form of a protonated alkyl ester of a carboxylic acid has carbonyl protonation, but the accepted decomposition path forming the protonated acid demands first 1,3 proton migration to the alkoxy oxygen followed by 1,5 hydrogen migration [23–26]. The proposed mechanism for the decomposition of protonated propyl acetate to protonated acetic acid and propene is shown here with energy changes computed from literature values [24].

The computed CBS-4M activation energy for 1,3 proton migration for both protonated propyl acetate, shown in Scheme 1, and

Table 1
Thermodynamic data for methyl acetate (M) (kJ mol^{-1}).

	Calculation	Experiment
Protonation on carbonyl	−844	−821.6[a]
Protonation on alkoxy	−769	
Dissociation of symmetrical M_2H^+	139	122[b]
Dissociation of asymmetrical M_2H^+	167	

[a] From Ref. [9].
[b] From Ref. [22].

protonated ethyl propanoate is 168 kJ mol^{-1}, considerably higher than the computed energy difference of 65 kJ mol^{-1} between the carbonyl and alkoxy protonated forms of the esters [26]. The computed barrier height for the 1,5 H atom migration is less than for the 1,3 shift but is greater by 17 kJ mol^{-1} for ethyl propanoate than for propyl acetate, a difference that is consistent with the relatively larger energy thresholds for F^+ formation shown by the ethyl esters in Fig. 7. The explanation is tenable however, only if the alkoxy protonated ester has a sufficiently long lifetime before it is activated to overcome the 1,5 hydrogen migration barrier. If this is not so, the second barrier, being at a significantly lower absolute energy than the first, has no bearing on the decomposition rate.

The observed increasing separation field requirement for the appearance of fragmentation of MH^+ with increasing mass seen in Fig. 7 is in agreement with a proton transfer reaction mass spectrometry study by Aprea et al. [27]. Esters were protonated by H_3O^+ and mass spectra were obtained after passage through a drift tube operating at 2.03 mbar with fields from 95 to 143 Td. The stability as a function of E/N of the protonated ethyl esters of acids, from acetic to decanoic, increased with increasing mass. This behavior was rationalized as due to the dissipation of the protonation energy, PA(ester)–PA(H_3O^+), among a greater number of bonds as the length of the acyl chain length increased, leading to an additional energy requirement from the electric field for MH^+ decomposition. The exoergicity of the protonation step is not a factor in our experiments but a similar argument holds. The nascent protonated esters are rapidly thermalized at atmospheric pressure to instrument temperature in the ion source region before encountering the separating field. The chain length does however still influence the field required for MH^+ decomposition due to the greater input of energy required to attain the same T_{eff} as the number of vibrational modes increases.

The reason why MH^+ disappears before M_2H^+ as the separation field is increased, observed at all temperatures for all the esters except methyl acetate, is not immediately obvious. The MH^+ decomposition product, the protonated carboxylic acid appears to come directly from M_2H^+ at fields when MH^+ is no longer observed. It is possible that sufficient energy is present in the dimer for both the dissociation to $MH^+ + M$ and for further decomposition of MH^+. However, this behavior is unlikely, especially at the threshold for decomposition since, as discussed above, an activated transfer of the proton from the carbonyl to the alkoxy oxygen in MH^+ is the first step. A second possibility might be that the bonding in M_2H^+ is changed as T_{eff} for M_2H^+ dissociation is approached. The lowest energy form of M_2H^+ has the proton between the two carbonyl oxygens and a change to a position between the carbonyl oxygen of one ester molecule and the alkoxy oxygen of the other would be required for simultaneous M_2H^+ dissociation and F^+ formation. The strength of the hydrogen bond in both forms of M_2H^+ was investigated by *ab initio* calculation of methyl acetate, which was chosen to decrease computational requirements.

A density functional theory calculation at the B3-LYP 6–311+G(d,p) level for methyl acetate produced the data shown in Table 1. No scaling factor for the fundamental vibrational frequencies was employed. The computed proton affinity for carbonyl protonation is 22 kJ mol^{-1} higher than the evaluated 821.6 kJ mol^{-1} [9] and the computed hydrogen bond energy for the symmetrical M_2H^+ is 17 kJ mol^{-1} higher than the experimental value of 122 kJ mol^{-1} [22]. This implies that all the calculated values shown in the table are all somewhat high. The proton affinity of alkoxy protonated methyl acetate is 75 kJ mol^{-1} lower than that of the carbonyl protonated form, consistent with the difference of 68 kJ mol^{-1} for both ethyl propanoate and propyl acetate obtained with the CBS-4M calculation [26]. The computed enthalpy difference between the symmetrical form of M_2H^+ with the proton between two carbonyl groups and the less stable asymmetrical form with the proton between a carbonyl group and an alkoxy group is 28 kJ mol^{-1}. This is much less than the hydrogen bond energy of 138 kJ mol^{-1} in the symmetrical dimer, so that at elevated temperatures the dimer may be a mixture of the symmetric and asymmetric forms. However, the asymmetrical dimer has the proton much closer to the carbonyl oxygen (1.021 Å) than to the alkoxy oxygen (1.588 Å) and so its dissociation, like that of the symmetrical dimer, would lead to the molecule protonated on the carbonyl oxygen. Formation of F^+ directly from the dimer is highly improbable.

A more likely explanation for the apparent direct decomposition of M_2H^+ to F^+ involves a mass dependence of energy uptake from the separation field to acquire a requisite T_{eff}. The energy gained by a singly charged ion in an electric field E over the average distance between collisions λ is $eE\lambda$. The centre of mass collision energy associated with an ion of mass m after collision with a gas molecule of mass M is $E_{cm} = eE\lambda M/(M+m)$ and the internal energy gained by the ion is always less than this [28]. If the assumption is made that the collision cross section is approximately the same for both M_2H^+ and MH^+ then the kinetic energy acquired by both ions is the same since the path length is the same. E_{cm} is lower for the heavier M_2H^+ leading to a lower energy input at the same electric field strength. For the same separation field strength it is therefore possible to attain a higher T_{eff} for MH^+ than for M_2H^+. When the separation field maximum intensity is high enough to dissociate M_2H^+, it is sufficiently higher than required for MH^+ dissociation, and this ion rapidly dissociates and only its product, F^+ is observed in the DMS spectrum.

4. Conclusions

Protonated n-alkyl carboxylic esters were decomposed in a differential mobility spectrometer to protonated carboxylic acid and alkene at effective temperatures determined by a combination of thermal energy and the energy produced by acceleration in a high radio frequency field. The minimum field for first observation of the product ion decreases by 0.68 Td for every 1° increase in instrument temperature i.e., 1 Td of high field heating raises the effective temperature of the decomposing ion by 1.5 °C. This effective temperature increase is, within experimental uncertainty, independent of ion identity for acetates. The minimum field increases with increasing size of the alkyl group at a given instrument temperature, consistent with a required higher energy input to attain the same effective temperature due to the increasing heat capacity.

The apparent decomposition of M_2H^+ to the protonated acid plus alkene without the appearance of MH^+ as an intermediate requires further investigation. The larger heat capacity of M_2H^+ relative to MH^+ would suggest that at given field and transport gas temperature the smaller ion attains a higher effective temperature. Comparison of these DMS results with those obtainable with a linear ion mobility spectrometer would enable the determination of T_{eff} for the decompositions. The thermal decomposition of some proton bound dimers in the drift tube [11] of a mobility spectrometer under low field conditions has been studied,

where the decomposition of $(DMP)_2H^+$ led only to the formation of $MH^+ + M$, as was found in this DMS study, and the same behavior was observed for the proton bound dimer of dimethyl methylphosphonate. Unfortunately, due to the lack of resolution between M_2H^+ and MH^+ the study of the decomposition of the dimer by DMS is not possible. Experiments are commencing in our laboratory to investigate the thermal decomposition of the MH^+ ions of alkyl esters by IMS for comparison with the DMS results that may allow an assignment of T_{eff} in their DMS decompositions. The experiments also include determinations of the rates of dissociation of proton bound dimers in a IMS drift tube designed to isolate M_2H^+ from other ions and neutrals prior to kinetic measurements.

References

[1] K.R. Jennings, Int. J. Mass Spectrom. 200 (1/3) (2000) 479–493.
[2] L. Drahos, K. Vekey, J. Mass Spectrom. 38 (2003) 1025–1042.
[3] A.V. Tomachev, A.N. Vilkov, B. Bogdanov, L. Pasa-Tolic, C.D. Masselon, R.D. Smith, J. Am. Soc. Mass Spectrom. 15 (2004) 1616–1628.
[4] G. Bouchoux, J. Mass Spectrom. 41 (8) (2006) 1006–1013.
[5] G.A. Eiceman, Z. Karpas, Ion Mobility Spectrometry, 2d edition, CRC Press, Boca Raton, FA, 2005.
[6] A.A. Schvartsburg, Differential Ion Mobility Spectrometry, CRC Press, Boca Raton, FA, 2009.
[7] S. Kendler, G.R. Lambertus, B.D. Dunietz, S.L. Coy, E.G. Nazarov, R.A. Miller, R.D. Sacks, Int. J. Mass Spectrom. 263 (2007) 137–147.
[8] M. Meot-Ner, A. Somogyi, Int. J. Mass Spectrom. 267 (2007) 346–356.
[9] NIST Chemistry WebBook, NIST Standard Reference Database Number 69, National Institute of Standards and Technology, Gaithersburg MD, 20899, http://webbook.nist.gov.
[10] R.G. Ewing, G.A. Eiceman, C.S. Harden, J.A. Stone, Int. J. Mass Spectrom. 255–256 (2006) 76–85.
[11] G.A. Eiceman, D.B. Shoff, C.S. Harden, A.P. Snyder, Int. J. Mass Spectrom. Ion Process. 85 (1988) 265–275.
[12] E.A. Mason, E.W. McDaniel, Transport Properties of Ions in Gases, Wiley, New York, 1988.
[13] I.A. Buryakov, E.V. Krylov, E.G. Nazarov, U.Kh. Rasulev, Int. J. Mass Spectrom. 128 (1993) 143–148.
[14] R.W. Purves, R. Guevremont, S. Day, C.W. Pipich, M.S. Matyjaszczyk, Rev. Sci. Instrum. 69 (1998) 4094–4105.
[15] B.M. Kolakowski, Z. Mester, Analyst 132 (9) (2007) 842–864.
[16] E. Krylov, E.G. Nazarov, R.A. Miller, B. Tadjikov, G.A. Eiceman, J. Phys. Chem. A 106 (2002) 5437–5444.
[17] N. Krylova, E. Krylov, G.A. Eiceman, J.A. Stone, J. Phys. Chem. A 107 (2003) 3648–3654.
[18] E.G. Nazarov, S.L. Coy, E.V. Krylov, R.A. Miller, G.A. Eiceman, Anal. Chem. 78 (2006) 7697–7706.
[19] G.A. Eiceman, E.G. Nazarov, R.A. Miller, Int. J. Ion Mobility Spectrom. 3 (2001) 15–27.
[20] J.W. Larson, T.B. McMahon, J. Am. Chem. Soc. 104 (1982) 6255–6261.
[21] M. Meot-Ner, J. Am. Chem. Soc. 106 (5) (1984) 1257–1264.
[22] J.E. Szulejko, T.B. McMahon, Int. J. Mass Spectrom. Ion Process. 109 (1991) 279–294.
[23] C.V. Pesheck, S.E. Buttrill, J. Am. Chem. Soc. 96 (1974) 6027–6032.
[24] A.C. Hopkinson, G.I. Mckay, D.K. Bohme, Can. J. Chem. 57 (1979) 2996–3004.
[25] J.A. Herman, A.G. Harrison, Can. J. Chem. 59 (1981) 2133–2145.
[26] G.J. Francis, D.B. Milligan, M.J. McEwan, J. Phys. Chem. A 111 (2007) 9670–9679.
[27] E. Aprea, F. Biasioli, T.D. Mark, F. Gasperi, Int. J. Mass Spectrom. 262 (2007) 114–121.
[28] J. Bordas-Nagy, K.R. Jennings, Int. J. Mass Spectrom. Ion Process. 100 (1990) 105–131.